

# Enhancement of persistent current in mesoscopic rings & cylinders : shortest & next possible shortest higher order hopping

Santanu K. Maiti\*, J. Chowdhury and S. N. Karmakar

*Saha Institute of Nuclear Physics, 1/AF, Bidhannagar, Kolkata 700 064, India*

## Abstract

We present a detailed study of persistent current and low-field magnetic susceptibility in single isolated normal metal mesoscopic rings and cylinders in the tight-binding model with higher order hopping integral in the Hamiltonian. Our exact calculations show that order of magnitude enhancement of persistent current takes place even in presence of disorder if we include higher order hopping integral in the Hamiltonian. In strictly one-channel mesoscopic rings the sign of the low-field currents can be predicted exactly even in presence of impurity. We observe that perfect rings with both odd and even number of electrons support only diamagnetic currents. On the other hand in the disordered rings, irrespective of realization of the disordered configurations of the ring, we always get diamagnetic currents with odd number of electrons and paramagnetic currents with even number of electrons. In mesoscopic cylinders the sign of the low-field currents can't be predicted exactly since it strongly depends on the total number of electrons,  $N_e$ , and also on the disordered configurations of the system. From the variation of persistent current amplitude with system size for constant electron density, we conclude that the enhancement of persistent current due to additional higher order hopping integrals are visible only in the mesoscopic regime.

**PACS No.:** 73.23.-b, 73.23.Ra, 73.20.Jc, 75.20.-g

**Keywords:** Higher Order Hopping, Persistent Current, Magnetic Susceptibility, Disorder

**\*Corresponding Author:**

Email address: santanu.maiti@saha.ac.in

# 1 Introduction

Since 1960 the study of magnetic response in normal metal mesoscopic loops provides many exotic new results as a consequence of phase coherence of the electrons in these small scale systems. Büttiker, Imry and Landauer [1] have shown following the works of Byers and Yang [2] that a small isolated normal metal ring threaded by slowly varying magnetic flux  $\phi$  carries an equilibrium current and it never decays, even in presence of impurity in the system. This current varies periodically with  $\phi$  showing  $\phi_0$  flux-quantum periodicity. Later experimental results have verified the existence of persistent current in such small rings. At very low temperatures, the inelastic scattering length is much larger than the ring size,  $L$ , and accordingly, the electron transport is completely phase coherent throughout the ring. Again in these small systems with finite size the energy levels are discrete. The large phase coherence length,  $L(\phi)$ , and the discreteness of the energy levels play an important role in the existence of persistent current in these normal metal loops. There are lots of theoretical studies [3, 4, 5, 6, 7, 8, 9, 10, 11, 12, 13] on persistent current in normal metal rings, but till now we are unable to explain many features of these currents that are observed experimentally. The experimental results on single isolated rings are significantly different from those for the ensemble of single isolated rings. The measured average currents are comparable to the sample-specific typical currents  $\langle I^2 \rangle^{1/2}$  predicted for a single ring, but are one or two orders of magnitude larger than the ensemble averaged persistent currents expected from free electron theory. The theoretical calculations including electron-electron interaction yield average persistent current within an order of magnitude of the experimental value, but cannot explain the diamagnetic sign of the currents. Levy *et al.* [14] have measured diamagnetic response of the currents at very low fields in an experiment on  $10^7$  isolated mesoscopic Cu rings. On the other hand, Chandrasekhar *et al.* [15] have determined  $\phi_0$  periodic currents in Ag rings with paramagnetic response at low fields. On the theoretical side, Cheung *et al.* [4] predicted that the direction of persistent current is random depending on the total num-

ber of electrons,  $N_e$ , in the system and the specific realization of the random potentials. Both diamagnetic and paramagnetic responses have been observed theoretically in mesoscopic Hubbard ring by Yu and Fowler [16]. They have shown that the rings with odd  $N_e$  exhibit paramagnetic response while those with even  $N_e$  give diamagnetic response in the limit  $\phi \rightarrow 0$ . In a recent experiment Jariwala *et al.* [17] obtained diamagnetic persistent currents with both  $\phi_0$  and  $\phi_0/2$  flux-quantum periodicities in an array of 30-diffusive mesoscopic gold rings. The diamagnetic sign of the currents in the vicinity of zero magnetic field were also found in an experiment [18] on  $10^5$  disconnected Ag ring. The sign is a priori not consistent with the theoretical predictions for the average of persistent current. Thus we see that theory and experiment still do not agree very well.

In this article we shall describe magnetic response of one-dimensional normal metal mesoscopic rings and cylinders within the one-electron picture using tight-binding Hamiltonian. All most all the existing theories are basically based on the framework of nearest-neighbor tight-binding Hamiltonian with either diagonal disorder or off-diagonal disorder. But here we consider an additional higher order hopping integral with the nearest-neighbor hopping (NNH) integral in the Hamiltonian and try to explain the dependences of persistent currents on the number of electrons  $N_e$ , disorder strengths  $W$ . We can consider higher order hopping integrals in the Hamiltonian on the basis that the overlap of the atomic orbitals between various neighboring sites are usually non-vanishing and the higher order hopping integrals become quite important. In this article we take only one higher order hopping integral, in addition to the NNH integral, which gives the hopping of an electron in the *next shortest path* between two sites. In case of strictly one-dimensional rings, i.e., rings with only one channel the next possible *shortest path* is equal to the twice of the lattice spacing (see Fig. 1), while, in cylinders it would be the diagonal distance (shown by the arrows in Fig. 7) of each small rectangular loop (see Fig. 7).

This paper is organized as follows. In section II, we study the variation of persistent current as a function of magnetic flux  $\phi$  in strictly one-dimensional meso-

scopic rings. Here we describe the dependences of persistent currents on electron numbers  $N_e$ , disorder strengths  $W$  and also on higher order hopping integral. Section III describes the behavior of persistent currents in mesoscopic cylinders and the effects of diagonal hopping integral on current in presence of impurity. The sign of the low-field currents in these mesoscopic rings and cylinders is clearly investigated in section IV. In section V, we compute the variation of current amplitudes with system size  $N$  both for one-channel mesoscopic rings and cylinders. Lastly, our conclusions are given in section VI.

## 2 One-dimensional Mesoscopic Ring

The Hamiltonian for a  $N$ -site ring in the tight-binding model can be written as,

$$H = \sum_i \epsilon_i c_i^\dagger c_i + \sum_{i \neq j} v_{ij} \left[ e^{i\theta_{ij}} c_i^\dagger c_j + h.c. \right] \quad (1)$$

where  $\epsilon_i$ 's are the site potential energies and the phase factors are  $\theta_{ij} = 2\pi\phi(|i-j|)/N$ . We take the hopping integral between any two sites  $i$  and  $j$ ,

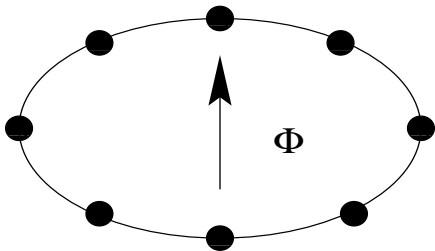


Figure 1: One dimensional normal metal ring threaded by a magnetic flux  $\phi$ . The filled circles denote the positions of the lattice site.

here in our present model  $j$  has the values  $i \pm 1$  and  $i \pm 2$  only, in the form  $v_{ij} = v \exp[\alpha(1 - |i - j|)]$ , where  $v$  is the hopping strength between any two nearest-neighbor sites. In this work we use the units  $c = e = \hbar = 1$ . As we are considering only non-magnetic impurities, the spin of the electrons will

not produce any qualitative change in the behavior of persistent current and low-field magnetic susceptibility, and so we neglect the spin of the electrons throughout this work.

At zero temperature, the persistent current is given by

$$I(\phi) = -\frac{\partial E(\phi)}{\partial \phi} \quad (2)$$

where  $E(\phi)$  is the ground state energy of the system. For a perfect ring we can calculate ground state energy analytically, while in a disordered ring we do exact numerical diagonalization to evaluate the ground state energy. Gauge invariance [2] implies that  $I(\phi)$  is a periodic function of  $\phi$  with period  $\phi_0 = ch/e = 1$ .

In this section we investigate the behavior of current-flux characteristics both for the ordered and disordered rings described by the Hamiltonians with only NNH integral and the rings described by the Hamiltonians with NNH integral in addition to the second neighbor hopping (SNH) integral. For an ordered ring we put  $\epsilon_i = 0$  for all  $i$  in the above Hamiltonian given by Eq. (1), and the energy of the  $n$ th single-particle state can be expressed as

$$E_n(\phi) = \sum_{p=1}^{p_0} 2 v \exp[\alpha(1-p)] \cos \left[ \frac{2\pi p}{N} (n + \phi) \right] \quad (3)$$

and the current carried by this eigenstate is

$$I_n(\phi) = \left( \frac{4\pi v}{N} \right) \sum_{p=1}^{p_0} p \exp[\alpha(1-p)] \times \sin \left[ \frac{2\pi p}{N} (n + \phi) \right] \quad (4)$$

where  $p$  is an integer. We take  $p_0 = 1$  and  $2$  respectively for the rings with NNH and SNH integrals.

At zero temperature, we can write the total persistent current in the following form

$$I(\phi) = \sum_n I_n(\phi) \quad (5)$$

where  $n$  is an integer and restricted in the range  $-[N_e/2] \leq n < [N_e/2]$  ( $[z]$  denotes the integer part of  $z$ ), where  $N_e$  denotes the number of electrons.

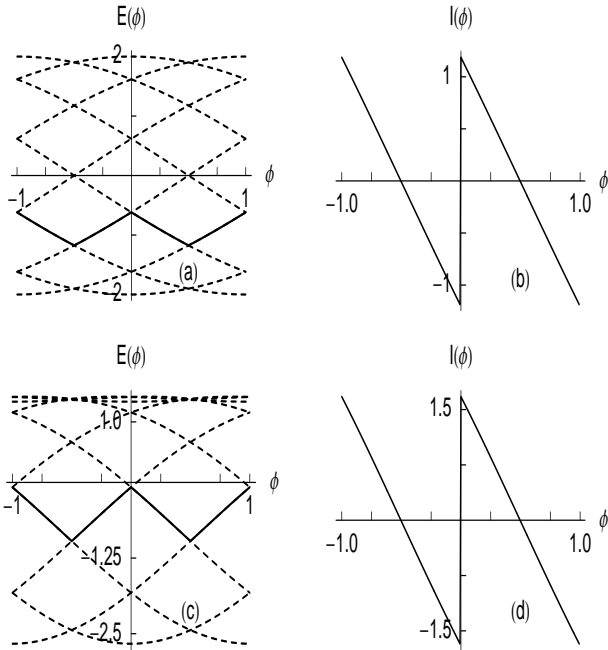


Figure 2: Energy spectra and persistent currents of 10-site perfect rings with four electrons ( $N_e = 4$ ), where a) and b) correspond to NNH model while c) and d) correspond to SNH ( $\alpha = 1.1$ ) model.

For large values of  $\alpha$ , the systems described by the SNH integral eventually reduce to the systems with only NNH integral. As we decrease the value of  $\alpha$ , contributions from the SNH integral become much more appreciable, and, the energy spectrum and persistent currents get modified, and these modifications give some new results both in absence and presence of disorder in the systems.

To reveal this fact, we first present in Fig. 2 the energy spectra and persistent currents of 10-site perfect rings with four electrons. The energy spectra for the NNH and SNH models are respectively shown in Fig. 2(a) and Fig. 2(c), and the solid curves give the variation of Fermi level at  $T = 0$  with flux  $\phi$ . We see that the SNH integral lowers the energy levels and most importantly below Fermi level the slopes of the  $E(\phi)$  versus  $\phi$  curves increases. As a result persistent

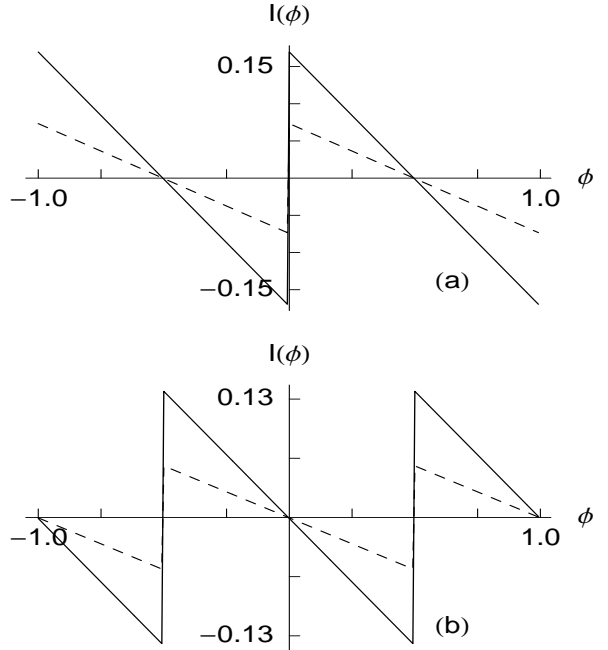


Figure 3: Persistent current as a function of  $\phi$  for ordered rings with  $N = 100$ ,  $\alpha = 0.9$ , and, a)  $N_e = 20$  and b)  $N_e = 15$ . The dotted and solid lines are respectively for the rings with NNH and SNH integrals.

current increases in the presence of SNH integrals and this enhancement of persistent current is clearly visible from Fig. 2(b) and Fig. 2(d). In Fig. 2 we have considered 10-site rings only for the sake of illustration and the results for the larger rings are presented in Fig. 3.

In Fig. 3 we plot  $I(\phi)$  versus  $\phi$  curves for some perfect rings with  $N = 100$  and  $\alpha = 0.9$ . The dotted and solid lines respectively gives the variation of current as a function of magnetic flux  $\phi$  for the systems with NNH and SNH integrals. The enhancement of current amplitudes due to the addition of SNH integral is clearly observed from Fig. 3(a) and Fig. 3(b) if we compare the results plotted by the dotted and solid curves. Fig. 3(a) shows that current has sharp transitions at  $\phi = 0$  or  $\pm n\phi_0$ , while, in Fig. 3(b) current shows the transitions at  $\phi = \pm n\phi_0/2$ . These

transitions are due to the degeneracy of the energy eigenstates at these respective fields. From Fig. 3 we see that for all the above models persistent currents are always periodic in  $\phi$  with  $\phi_0$  flux periodicity.

To understand the role of higher order hopping integral on persistent currents in disordered rings, we first study the energy spectra and currents in small rings, and the results for 10-site rings with  $N_e = 4$  are shown in Fig. 4. We describe the system by Hamiltonian Eq. (1) with site energies  $\epsilon_i$ 's chosen randomly between  $-W/2$  to  $W/2$ , where  $W$  being the strength of disorder. In Fig. 4(a) and Fig. 4(c) we present the

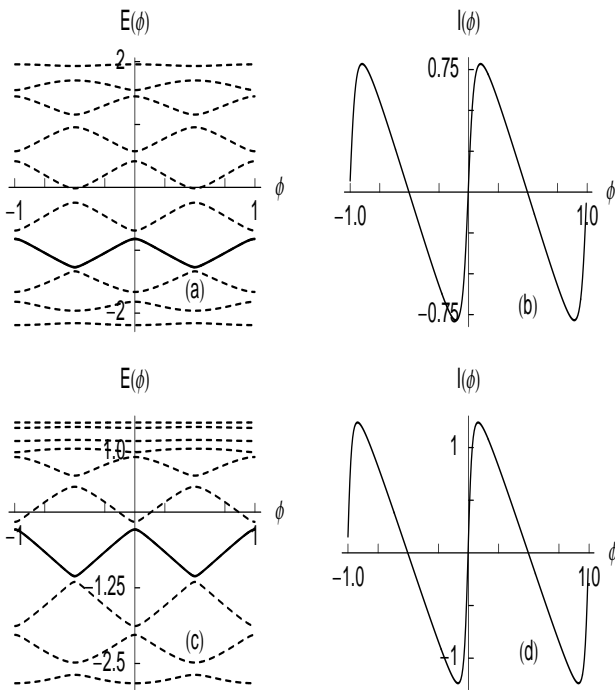


Figure 4: Energy spectra and persistent currents of 10-site disordered ( $W = 1$ ) rings with four electrons ( $N_e = 4$ ), where a) and b) correspond to NNH model while c) and d) correspond to SNH ( $\alpha = 1.1$ ) model.

energy spectra respectively for the NNH and SNH models where solid curves give the location of the Fermi level. As in the ordered situations, the SNH integral lowers the energy levels and below Fermi level

the slopes of the  $E(\phi)$  versus  $\phi$  curves are much more than those for the NNH model. Thus even in the presence of disorder, we have enhancement of persistent current due to SNH integral.

The results for the larger disordered rings are given in Fig. 5 where we take  $N = 100$ ,  $\alpha = 0.9$  and  $W = 1$ . The persistent currents corresponding to the cases with NNH and SNH integrals are respectively represented by the dotted and solid lines. Here results are presented for some typical disordered configurations of the ring and in fact, we observe that the qualitative behavior of the persistent currents do not depend on the specific realization of the disordered configura-

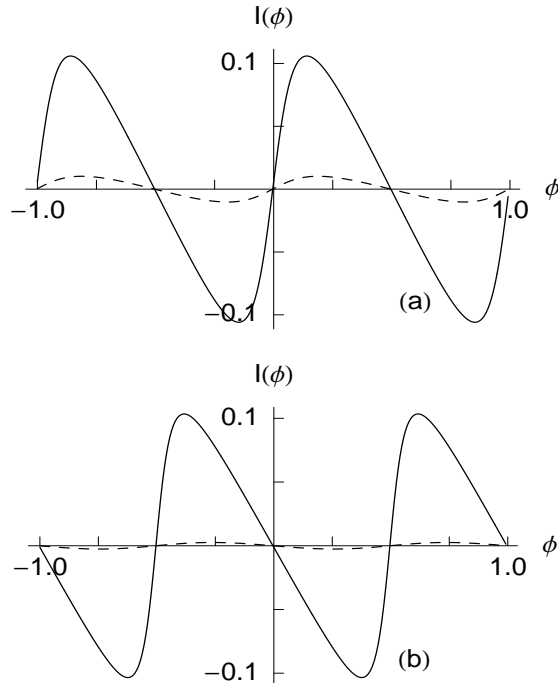


Figure 5: Persistent current as a function of  $\phi$  for the disordered rings with  $N = 100$ ,  $\alpha = 0.9$ ,  $W = 1$ , and, a)  $N_e = 20$  and b)  $N_e = 15$ . The dotted and solid lines are respectively for the rings with NNH and SNH integrals.

tions. This figure shows that the persistent currents for the disordered rings are always periodic in  $\phi$  with

$\phi_0$  flux periodicity. In the presence of disorder, we see from Fig. 5 that the persistent current always becomes a continuous function of magnetic flux  $\phi$ , and this behavior can be understood as follows (see Ref. [19]). The sharp transitions at the points  $\phi = 0$  or  $\pm n\phi_0$  with even  $N_e$  and at  $\phi = \pm n\phi_0/2$  with odd  $N_e$ , for the perfect rings (see Fig. 3) appear due to the degeneracy of the ground state energy at these

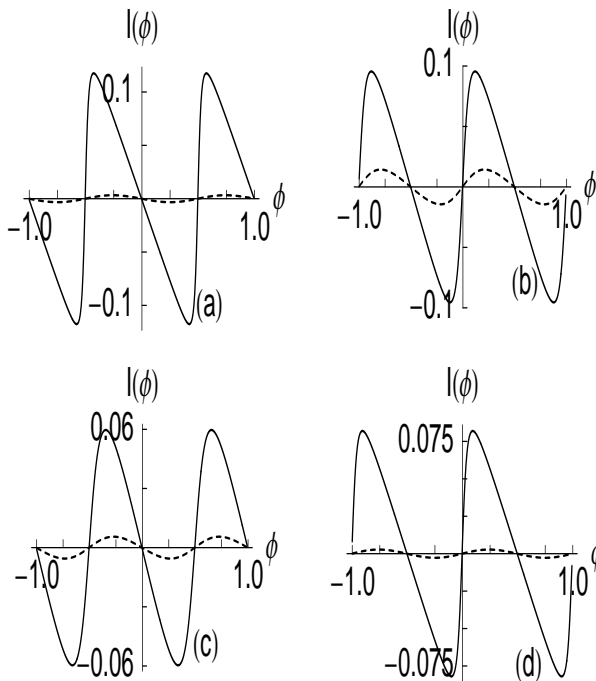


Figure 6: Persistent current as a function of  $\phi$  for different disordered ( $W = 1$ ) rings with higher electron concentrations. Here we choose  $\alpha = 1.1$ . a)  $N = 125$ ,  $N_e = 45$ ; b)  $N = 125$ ,  $N_e = 40$ ; c)  $N = 150$ ,  $N_e = 55$  and d)  $N = 150$ ,  $N_e = 60$ .

points. Now as the impurities are introduced, all the degeneracies get lifted and current exhibits a continuous variation with respect to  $\phi$ . At these degenerate points, the ground state energy passes through an extrema which in turn gives zero persistent current as shown in Fig. 5. It is clear from Fig. 5 that the higher order hopping integral play an important role to en-

hance the amplitude of persistent current in the disordered rings. From Fig. 5(a) and Fig. 5(b) we see that the currents in the disordered rings with only NNH integrals (the dotted lines) are vanishingly small compared to those as observed in the impurity free rings with NNH integrals (the dotted curves in Fig. 3(a) and Fig. 3(b)). On the other hand, Fig. 5 shows that the persistent currents in the disordered rings with higher order hopping integral are of the same order of magnitude as those for the ordered rings.

In Fig. 6 we give persistent currents for the disordered rings with higher electron concentrations and study the cases with  $N =$  even or odd and  $N_e =$  even or odd. The dotted and solid curves respectively corresponds to the NNH and SNH models. It is observed that the evenness or the oddness of  $N$  and  $N_e$  do not play any important role on persistent current but we will see that the diamagnetic or paramagnetic sign of persistent current crucially depends on the evenness or oddness of  $N_e$ .

Physically, the higher order hopping integrals try to delocalize the energy eigenstates and thereby favor phase coherence of the electrons even in the presence of disorder, and thus prevents the reduction of persistent current due to disorder. While in the disordered rings with only NNH integrals, the enormous reduction of current amplitudes are basically due to localization of the energy eigenstates. When we add higher order hopping integrals, it is most likely that the localization length increases and may become comparable to the length of the ring, and, we get enhancement of persistent current.

### 3 Mesoscopic Cylinder

This section investigates the behavior of persistent currents as a function of magnetic flux  $\phi$  both in perfect and dirty multi-channel mesoscopic cylinders described respectively by NNH and SNH (diagonal hopping shown by the arrows in Fig. 7) integrals. The main motivation for the study of the characteristic behaviors of persistent current in these mesoscopic cylinders is that, due to the existence of multi-channels, there is a possibility of diffusion of the electrons in presence of impurity and the enhancement of

persistent current in diffusive systems can be clearly verified.

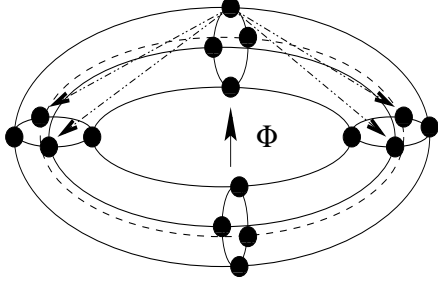


Figure 7: A normal metal mesoscopic cylinder threaded by a magnetic flux  $\phi$ . The filled circles correspond the positions of the lattice site.

The tight-binding Hamiltonian of such a multi-channel mesoscopic cylinder threaded by a magnetic flux  $\phi$  with  $N$  and  $M$  number of sites respectively along the longitudinal and transverse direction can be written in the following form

$$\begin{aligned}
H = & \sum_l \epsilon_l c_l^\dagger c_l + \sum_t \epsilon_t c_t^\dagger c_t + \sum_{\langle t, t' \rangle} v_{tt'} c_t^\dagger c_{t'} \\
& + \sum_{\langle l, l' \rangle} \left[ v_{ll'} e^{i\theta_{ll'}} c_l^\dagger c_{l'} + h.c. \right] \\
& + \sum_{\langle d, d' \rangle} \left[ v_{dd'} e^{i\theta_{dd'}} c_d^\dagger c_{d'} + h.c. \right] \quad (6)
\end{aligned}$$

where,  $\epsilon_l$  and  $\epsilon_t$  are the site potential energies along the longitudinal and transverse direction respectively.  $v_{tt'}$  is the transverse hopping strength, while,  $v_{ll'}$  and  $v_{dd'}$  respectively corresponds the hopping strength along the longitudinal and diagonal direction. The phase factors  $\theta_{ll'}$  and  $\theta_{dd'}$  are identical with  $(2\pi\phi/N)$  and the diagonal hopping strength  $v_{dd'} = v \exp(-\alpha)$ ,  $v$  is the NNH strength along the longitudinal direction.

Here we focus the behavior of persistent current for perfect and dirty cylindrical systems considering both NNH and SNH integrals. For a perfect cylinder, taking  $\epsilon_l = 0$  for all  $l$  and  $\epsilon_t = 0$  for all  $t$ , the energy eigenvalue of  $n$ th eigenstate is expressed in the form

$$E_n(\phi) = 2 v \cos \left[ \frac{2\pi}{N} (n + \phi) \right]$$

$$\begin{aligned}
& + 4 v \exp(-\alpha) \cos \left[ \frac{2\pi}{N} (n + \phi) \right] \times \\
& \cos \left[ \frac{2\pi m}{M} \right] + 2 v \cos \left[ \frac{2\pi m}{M} \right] \quad (7)
\end{aligned}$$

and the corresponding persistent current carried by this eigenstate is given by

$$\begin{aligned}
I_n(\phi) = & \left( \frac{4\pi v}{N} \right) \sin \left[ \frac{2\pi}{N} (n + \phi) \right] \\
& + \left( \frac{8\pi v}{N} \right) \exp(-\alpha) \sin \left[ \frac{2\pi}{N} (n + \phi) \right] \times \\
& \cos \left[ \frac{2\pi m}{M} \right] \quad (8)
\end{aligned}$$

where  $n$  and  $m$  are two integers respectively bounded within the range :  $-[N/2] \leq n < [N/2]$  and  $-[M/2] \leq m < [M/2]$ .

Now try to explain the behavior of persistent current in multi-channel cylindrical systems described by NNH integral only. As representative examples we plot the results of persistent current in these systems in Fig. 8. Here we consider the ring size  $N = 50$  along the longitudinal direction and  $M = 4$  along the transverse direction. The results shown in Fig. 8(a) and Fig. 8(b) are respectively for the cylinders with  $N_e = 45$  and  $N_e = 40$  where the solid lines correspond the variation of persistent current in absence of any impurity ( $W = 0$ ) and the dotted lines correspond those results for the dirty systems with disorder strength  $W = 1$ . Now in these multi-channel perfect systems current shows several kink-like structures (see solid curves in Fig. 8(a) and Fig. 8(b)) at different values of  $\phi$ , depending on  $N_e$ , compared to the results for one-channel perfect rings (see the curves in Fig. 3(a) and Fig. 3(b)). This is due to the fact that in multi-channel systems several additional overlaps of the energy levels take place compared to the one-channel systems. But the current always gets  $\phi_0$  flux-quantum periodicity. As the impurities are switched on all the degeneracies go out and current gets a continuous variation as shown by the dotted curves in Fig. 8(a) and Fig. 8(b). For these cylindrical systems described by NNH integral only it is observed that in presence of disorder current amplitude gets reduced by an order of magnitude compared to the current amplitude in perfect systems.

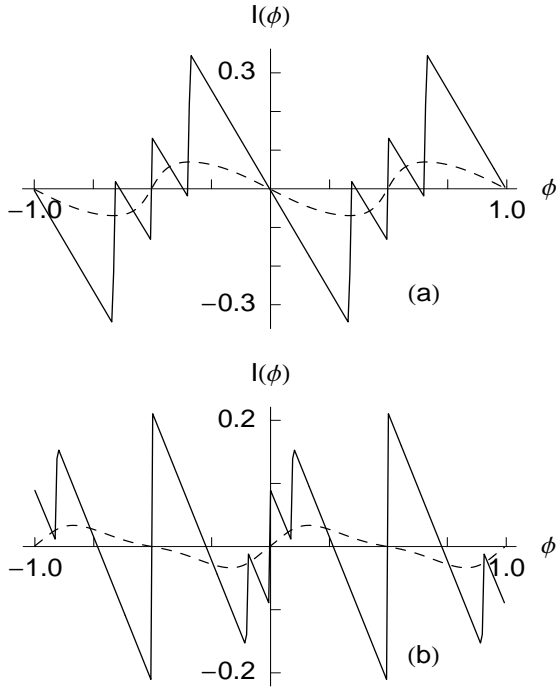


Figure 8: Persistent current as a function of  $\phi$  for multi-channel mesoscopic cylinders described by only NNH integral with  $N = 50$ ,  $M = 4$ , and, a)  $N_e = 45$  and b)  $N_e = 40$ . The solid and dotted lines are respectively for perfect ( $W = 0$ ) and dirty ( $W = 1$ ) cylinders.

Now we focus our attention on the behavior of persistent current for the multi-channel cylindrical systems described with both NNH and SNH integrals. In Fig. 9(a) and Fig. 9(b) we display the variation of persistent currents as a function of  $\phi$  for the multi-channel mesoscopic cylinders in presence of SNH ( $\alpha = 1.0$ ) integral in addition to the NNH integral taking the same system size ( $M = 50$  and  $N = 4$ ) as in the systems described with NNH integral only. The results shown in Fig. 9(a) and Fig. 9(b) are respectively for the systems with  $N_e = 45$  and  $N_e = 40$  where the solid curves present the results of perfect ( $W = 0$ ) cylinders and the dotted curves give the results of dirty ( $W = 1$ ) cylinders. From the curves

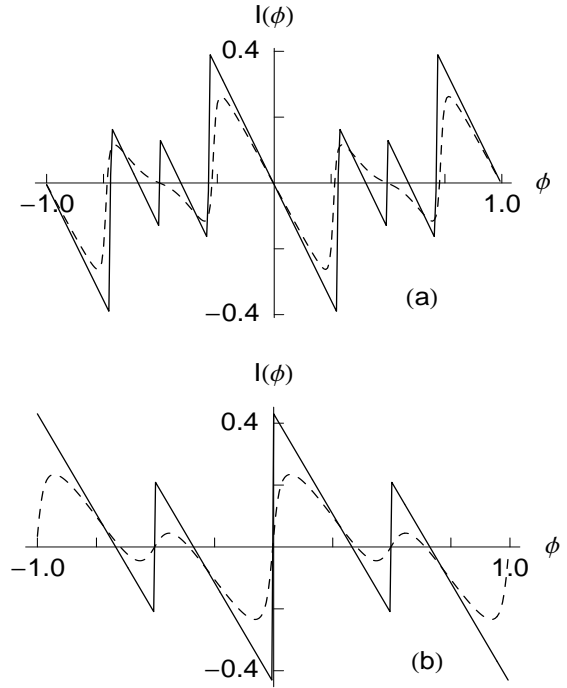


Figure 9: Persistent current as a function of  $\phi$  for multi-channel mesoscopic cylinders described by both NNH and SNH ( $\alpha = 1.0$ ) integrals with  $N = 50$ ,  $M = 4$ , and, a)  $N_e = 45$  and b)  $N_e = 40$ . The solid and dotted curves are respectively for perfect ( $W = 0$ ) and dirty ( $W = 1$ ) cylinders.

shown in Fig. 9(a) and Fig. 9(b) we can emphasize that current amplitudes in dirty systems (see dotted curves) are comparable to that of perfect systems (see solid curves). This is due to the fact that higher order hopping integrals try to delocalize the energy eigenstates and thus current amplitude increases, even an order of magnitude, in comparison with the current amplitude in dirty cylinders described with NNH integral only.

Thus our results for both one-channel mesoscopic rings and multi-channel mesoscopic cylinders predict that higher order hopping integral has an important role for the enhancement of current amplitude in presence of impurity.

## 4 Low-field Magnetic Susceptibility

In this section we address the behavior of low-field magnetic susceptibility for both the ordered and disordered one-channel mesoscopic rings and multi-channel cylinders described by the Hamiltonians with NNH and SNH integrals. This quantity can be cal-

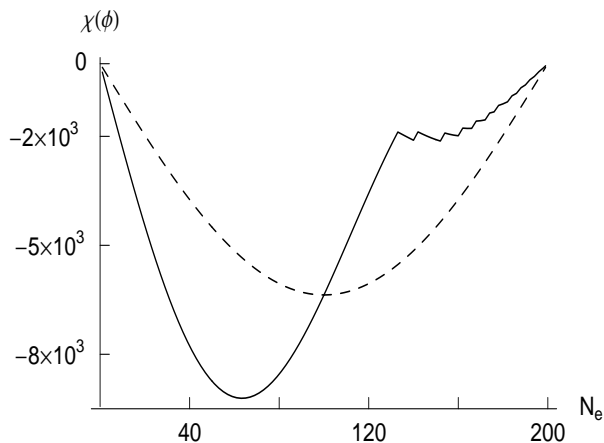


Figure 10:  $\chi$  versus  $N_e$  curves near zero-field for ordered rings with  $N = 200$  and  $\alpha = 1.1$ . The dotted and solid lines are respectively for the rings with NNH and SNH integrals.

culated from the first order derivative of persistent current and the general expression of magnetic susceptibility is of the form

$$\chi(\phi) = \frac{N^3}{16\pi^2} \left( \frac{\partial I(\phi)}{\partial \phi} \right) \quad (9)$$

Calculating magnetic susceptibility we can precisely predict the diamagnetic and paramagnetic signs of the persistent currents in such systems [14, 15, 16, 17, 18]. Our calculations for strictly one-channel rings show that the sign of the persistent current is not a random quantity, rather it is independent of the specific realizations of disorder, while, the calculations for multi-channel cylinders emphasize that the sign of the currents cannot be predicted

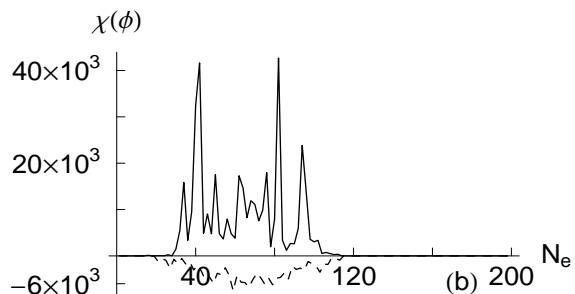
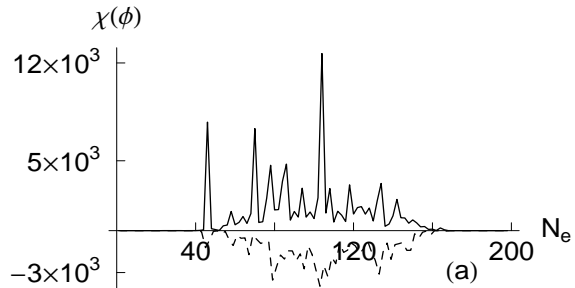


Figure 11:  $\chi$  versus  $N_e$  curves near zero-field for disordered rings with  $N = 200$ ,  $\alpha = 1.1$  and  $W = 1$ . The results corresponding to the Hamiltonians with NNH and SNH integrals are respectively presented in a) and b). The solid and dotted lines are respectively for the rings with even and odd  $N_e$ .

precisely since it strongly depends on the total number of electrons,  $N_e$ , and also on the specific realization of disordered configurations of the system.

Let us first try to describe the sign of the low-field currents in strictly one-channel mesoscopic rings. In a perfect ring, the magnetic susceptibility associated with the current  $I_n(\phi)$  carried by  $n$ th eigenstate can be expressed as

$$\chi_n(\phi) = \frac{N}{4} \sum_{p=1}^{p_0} 2 v p^2 \exp[\alpha(1-p)] \times \cos \left[ \frac{2\pi p}{N} (n + \phi) \right] \quad (10)$$

At zero temperature the total magnetic susceptibility will be  $\chi(\phi) = \sum_n \chi_n(\phi)$ , where the summation over the quantum number  $n$  lies in the range  $-[N_e/2] \leq n < [N_e/2]$ . In Fig. 10, we display the variation of low-field magnetic susceptibility of perfect rings with the number of electrons  $N_e$  in the rings. The dotted and solid curves respectively correspond the rings described by the Hamiltonians with NNH and SNH integrals. These two curves indicate that in the limit  $\phi \rightarrow 0$ , persistent current exhibits a diamagnetic sign irrespective of the total number of electrons,  $N_e$ , in the rings. This diamagnetic sign of the currents follows from the slope of the curves at the zero field limit ( $\phi \rightarrow 0$ ) presented in Fig. 3. So we conclude that at low magnetic fields ( $\phi \rightarrow 0$ ), there will be only diamagnetic persistent currents in perfect rings.

Now we investigate the behavior of low-field magnetic susceptibility for the disordered rings. In Fig. 11 we plot the low-field magnetic susceptibility as a function of  $N_e$  for the rings taking the ring size  $N = 200$  and disorder strength  $W = 1$ . The results for the models with NNH and SNH integrals are displayed respectively in Fig. 11(a), and Fig. 11(b) considering  $\alpha = 0.9$ . The solid and dotted lines in these figures are respectively for the rings with even and odd number of electrons,  $N_e$ . The curves in Fig. 11 correspond to some typical disordered configurations of the rings. The most interesting finding is that the persistent currents in the disordered rings always show diamagnetic sign for odd  $N_e$  and paramagnetic sign for even  $N_e$ . At low fields the  $I - \phi$  curves for the perfect rings have a discontinuity when  $N_e$  is even whereas for odd  $N_e$  there is no discontinuity (see Fig. 3), but in both the cases persistent currents have diamagnetic sign. As disorder removes the discontinuity of the  $I - \phi$  curves, the slopes of the  $I - \phi$  curves near zero field become positive for even  $N_e$  while the slopes remain negative for odd  $N_e$  (see Fig. 5). This has a very general consequence that irrespective of the disordered configurations, at low fields we always get diamagnetic persistent current when  $N_e$  is odd and paramagnetic current when  $N_e$  is even.

Finally, let us consider the behavior of the sign of persistent currents for the mesoscopic multi-channel cylinders in the limit  $\phi \rightarrow 0$ . In absence of any impurity i.e., for perfect cylinders the magnetic suscepti-

bility associated with the current  $I_n(\phi)$  carried by  $n$ th energy eigenstate considering both NNH and SNH (diagonal hopping which is shown by the arrows in Fig. 7) integrals is written in the form

$$\chi_n(\phi) = \frac{Nv}{2} \left\{ \cos \left[ \frac{2\pi}{N}(n + \phi) \right] + 2 \exp(-\alpha) \times \cos \left[ \frac{2\pi}{N}(n + \phi) \right] \cos \left[ \frac{2\pi m}{M} \right] \right\} \quad (11)$$

In these cylindrical systems the sign of the low-field currents cannot be predicted exactly, even in absence of any impurity, since the sign of the currents strongly depends on the total number of electrons,  $N_e$ , and for dirty systems it also strongly depends on the specific realization of disordered configurations.

## 5 Magnitude of Persistent Current Amplitude with System Size $N$

In this section we show that the higher order hopping integrals play an important role to enhance persistent current in the disordered mesoscopic rings and cylinders. For this purpose we study the behavior of persistent current with system size  $N$  in these systems for constant electron density, i.e., for constant  $N_e/N$  ratio. We have calculated the current amplitude  $I_0$  at some typical field, say at  $\phi = 0.25$ , and the  $I_0$  versus  $N$  curves are shown in Fig. 12. The results for the rings described with NNH integral only are plotted in Fig. 12(a), while those for the rings described by NNH and SNH integrals are shown in Fig. 12(b) keeping the ratio  $N/N_e = 2$  in both the cases. The dotted and solid lines correspond to the rings in absence of any impurity ( $W = 0$ ) and in presence of impurity with strength  $W = 1$  respectively. If we compare Fig. 12(a) and Fig. 12(b), we see that the currents in the disordered rings are orders of magnitude less than those for the perfect rings at the mesoscopic length scale when we use the model with only NNH integrals (see dotted curve in Fig. 12(a)). Quite interestingly we observe that when the SNH integrals are switched on in addition to the NNH integrals in the

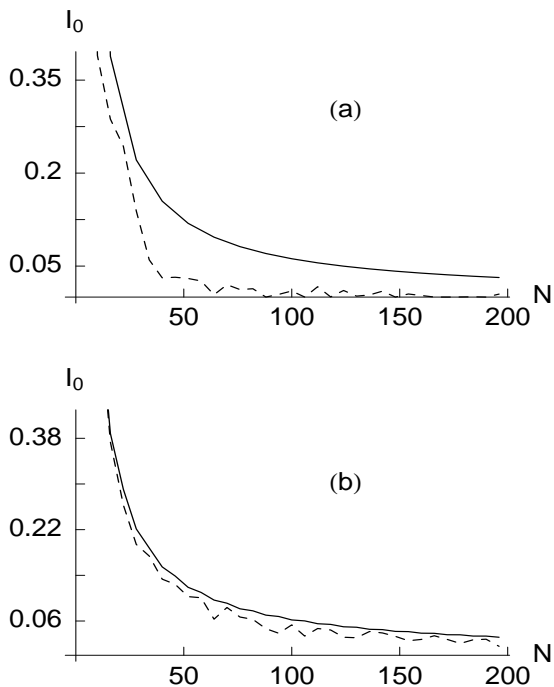


Figure 12: Current amplitude  $I_0$  as a function of system size  $N$  in one-channel mesoscopic rings keeping the ratio  $N_e/N$  as a constant by the relation  $N = 2N_e$ , where (a) rings described with NNH integral only and (b) rings described with both NNH and SNH ( $\alpha = 0.9$ ) integrals. The dotted and solid lines respectively corresponds the results for perfect and dirty ( $W = 1$ ) systems.

disordered rings, the current amplitudes have some finite non-zero values, comparable to the perfect ring results, even if  $N$  is in the mesoscopic regime and this is evident from the dotted curve of Fig. 12(b).

In multi-channel mesoscopic cylinders, keeping  $N_e/N$  ratio as a constant, we also get the similar kind of behavior for the amplitude variation.

In the nearest-neighbor tight-binding model, disorder tries to localize the electrons and the persistent current becomes almost zero at the mesoscopic length scale. On the other hand, in the presence of higher order hopping integrals the electron eigenstates are not localized within the mesoscopic length scale, and we get enhanced persistent current as the electronic phase coherence is preserved over the sample size. Accordingly, we can emphasize that both for one-channel mesoscopic rings and multi-channel mesoscopic cylinders the higher order hopping integrals have an important role for the enhancement of persistent current amplitude.

## 6 Conclusion

In conclusion, we have studied in details the characteristic behavior of persistent current and low-field magnetic susceptibility in one-channel mesoscopic rings and multi-channel mesoscopic cylinders within the tight-binding framework in presence of higher order hopping integrals. We have shown that the addition of higher order hopping integrals in the nearest-neighbor tight-binding Hamiltonian gives order of magnitude enhancement of persistent current in the disordered mesoscopic rings and cylinders. In this paper we have also calculated low field magnetic susceptibility of these systems as a function of  $N_e$ , and our exact calculations for one-channel rings show that the sign of the current is independent of the realization of disorder, it can be diamagnetic or paramagnetic depending on whether  $N_e$  is odd or even, while the calculations for the multi-channel mesoscopic cylinders indicate that the sign of the low-field currents cannot be predicted, even in absence of any impurity, since it strongly depends on  $N_e$  and for dirty cylinders it also depends on the specific realization of disordered configurations. From the variation of

current amplitude with system size  $N$  for constant electron density, we see that enhancement of persistent current due to higher order hopping integrals will be appreciable only in the mesoscopic scale.

## References

- [1] M. Büttiker, Y. Imry, and R. Landauer, Phys. Lett. **96A**, 365 (1983).
- [2] N. Byers and C. N. Yang, Phys. Rev. Lett. **7**, 46 (1961).
- [3] H. F. Cheung, Y. Gefen, E. K. Riedel, and W. H. Shih, Phys. Rev. B **37**, 6050 (1988).
- [4] H. F. Cheung and E. K. Riedel, Phys. Rev. Lett. **62**, 587 (1989).
- [5] G. Montambaux, H. Bouchiat, D. Sigeti, and R. Friesner, Phys. Rev. B **42**, 7647 (1990).
- [6] B. L. Altshuler, Y. Gefen, and Y. Imry, Phys. Rev. Lett. **66**, 88 (1991).
- [7] F. von Oppen and E. K. Riedel, Phys. Rev. Lett. **66**, 84 (1991).
- [8] A. Schmid, Phys. Rev. Lett. **66**, 80 (1991).
- [9] V. Ambegaokar and U. Eckern, Phys. Rev. Lett. **65**, 381 (1990).
- [10] M. Abraham and R. Berkovits, Phys. Rev. Lett. **70**, 1509 (1993).
- [11] G. Bouzerar, D. Poilblanc, and G. Montambaux, Phys. Rev. B **49**, 8258 (1994).
- [12] T. Giamarchi and B. S. Shastry, Phys. Rev. B **51**, 10915 (1995).
- [13] Santanu K. Maiti, J. Chowdhury, and S. N. Karmakar, Phys. Lett. A **332**, 497 (2004).
- [14] L. P. Levy, G. Dolan, J. Dunsmuir, and H. Bouchiat, Phys. Rev. Lett. **64**, 2074 (1990).
- [15] V. Chandrasekhar, R. A. Webb, M. J. Brady, M. B. Ketchen, W. J. Gallagher, and A. Kleinsasser, Phys. Rev. Lett. **67**, 3578 (1991).
- [16] N. Yu and M. Fowler, Phys. Rev. B **45**, 11795 (1992).
- [17] E. M. Q. Jariwala, P. Mohanty, M. B. Ketchen, and R. A. Webb, Phys. Rev. Lett. **86**, 1594 (2001).
- [18] R. Deblock, R. Bel, B. Reulet, H. Bouchiat, and D. Maily, Phys. Rev. Lett. **89**, 206803 (2002).
- [19] Santanu K. Maiti, J. Chowdhury, and S. N. Karmakar, Solid State Commun. **135**, 278 (2005).